

Geometric mass acquisition via quantum metric: an effective band mass theorem for the helicity bands

M. Iskin

Department of Physics, Koç University, Rumelifeneri Yolu, 34450 Sarıyer, Istanbul, Turkey

(Dated: April 16, 2019)

By taking the virtual inter-band transitions along with the intra-band ones into full account, here we first propose an effective band mass theorem that is suitable for a wide-class of single-particle Hamiltonians exhibiting multiple energy bands. Then, for the special case of two-band systems, we show that the inter-band contribution to the effective band mass of a particle at a given quantum state is directly controlled by the quantum metric of the corresponding state. As an illustration, we consider a spin-orbit coupled spin-1/2 particle and calculate its effective band mass at the band minimum of the lower helicity band. Independent of the coupling strength, we find that the bare mass m_0 of the particle jumps to $2m_0$ for the Rashba and to $3m_0$ for the Weyl coupling. This geometric mass enhancement is a non-perturbative effect, uncovering the mystery behind the effective mass of the two-body bound states in the non-interacting limit. As a further illustration, we show that a massless Dirac quasiparticle acquires a linearly dispersing band mass (equivalent to the effective cyclotron mass up to a prefactor) with its momentum through the same mechanism.

Introduction. Depending on the physical context, the helicity of a particle may refer to the projection of its orbital and/or spin angular momentum onto the direction of its center of mass motion, e.g., the helicity is said to be right (or left) handed when the relevant quantities are aligned (or anti-aligned). One of the central themes in a wide-range of modern single-, two-, few- or many-body physics problems is the so-called spin-orbit coupling (SOC), as it has found a plethora of interdisciplinary applications across atomic and molecular, particle, high-energy, nuclear, solid-state and condensed-matter physics, spreading over many decades. A great deal of these problems involve a $\mathbf{d}_{\mathbf{k}} \cdot \boldsymbol{\sigma}$ like \mathbf{k} -dependent Zeeman term in the equations of motion, where the motional degrees of freedom is described by some vector field $\mathbf{d}_{\mathbf{k}}$ that depends on the linear momentum $\mathbf{p} = \hbar\mathbf{k}$ through the wave vector \mathbf{k} , and $\boldsymbol{\sigma}$ is a vector of spin matrices corresponding to the spin or generally pseudo-spin (e.g., sublattice, hyperfine, valley, etc.) degrees of freedom. For instance, the generic coupling $\hbar \sum_i \alpha_i k_i \sigma_i$ is widespread in physics literature, describing cold atoms in artificial non-Abelian gauge fields [1–11], Dirac electrons in low-energy excitations of graphene [12–14], and Dirac quasiparticles at the surface of three dimensional topological insulators [15, 16], organic quasi-two-dimensional materials [17], and artificial honeycomb like (e.g., optical [18], molecular [19], microwave [20], etc.,) crystals.

Given the foremost importance of the spin-momentum coupling for the general physics community, here we develop a so-called *effective band mass theorem* for the helicity bands that is suitable for a wide-class of single-particle Hamiltonians. Our theorem has two physically distinct components: in addition to the usual contribution coming from the intra-band transitions, there is a geometric contribution stemming from the virtual inter-band ones controlled by the quantum metric of the corresponding quantum state. As an illustration, first we

consider a spin-orbit coupled spin-1/2 particle, and calculate its effective band mass at the band minimum of the lower helicity band. It turns out that the bare mass m_0 of the particle jumps to $2m_0$ for the Rashba and to $3m_0$ for the Weyl coupling independently of the coupling strength, i.e., the geometric mass enhancement is a non-perturbative effect. Since the quantum metric effects are both rare and elusive in nature [21–36], the experimental verification of these predictions with the recently realized Rashba like SOCs [8–11] would be an important leap towards the geometric and topological interpretations of quantum mechanics [37–39]. As a further illustration, then we apply the theorem to a massless Dirac quasiparticle, showing that the acquired geometric band mass of the particle disperses linearly with its momentum.

It is important to emphasize that the quantum metric contribution to the effective band mass of a single particle unveiled in this paper is distinct from our recent findings on a counterpart effect on the effective mass of many-body (Cooper pairs) as well as two-body (molecular) bound states throughout the BCS-BEC crossover in superfluid Fermi gases [33, 34]. These previous works revealed that, through dressing the effective mass of the relevant bound state, the quantum metric governs not only the superfluid density of some flat-band [31, 32] and two-band [33, 35] Fermi superfluids exhibiting non-trivial quantum geometry, but also many other observables including the sound velocity and spin susceptibility [36]. Unlike all of these previous works on Fermi superfluids where the quantum metric is integrated over \mathbf{k} space with some additional weight factors, this work paves the direct way towards measuring a local and non-perturbative quantum metric effect on either pseudo-spin-1/2 Fermi [8, 9] or Bose [10, 11] gases, independently of the particle statistics.

Effective band mass theorem for multi-band Hamiltonians. Having multiple bands in mind, we consider a

generic band structure that is determined by the wave equation $H_{\mathbf{k}}|n\mathbf{k}\rangle = \varepsilon_{n\mathbf{k}}|n\mathbf{k}\rangle$, where $H_{\mathbf{k}}$ is the single-particle Hamiltonian density in reciprocal space, and $|n\mathbf{k}\rangle$ and $\varepsilon_{n\mathbf{k}}$ denote, respectively, the corresponding energy eigenstates and eigenvalues. Here, the quantum states are labeled by the band index n and wave vector \mathbf{k} . In the presence of such a multi-band setting, the conventional wisdom [40] for the definitions of the effective band velocity $\mathbf{v}_{n\mathbf{k}}$ and effective band mass tensor $\mathbb{M}_{n\mathbf{k}}$ of a particle is such that they are determined by the coefficients of the linear and quadratic terms in the following small- \mathbf{q} expansion

$$\varepsilon_{n,\mathbf{k}+\mathbf{q}} = \varepsilon_{n\mathbf{k}} + \hbar \sum_i v_{n\mathbf{k}}^i q_i + \frac{\hbar^2}{2} \sum_{ij} [\mathbb{M}_{n\mathbf{k}}^{-1}]^{ij} q_i q_j + \dots$$

Thus, both the components $v_{n\mathbf{k}}^i$ of the velocity and the eigenvalues $M_{n\mathbf{k}}^P$ of the mass tensor along the principal axes may have strong dependence on \mathbf{k} that is controlled by the microscopic details of a given system.

Noting that $\varepsilon_{n,\mathbf{k}+\mathbf{q}}$ is an energy eigenvalue of $H_{\mathbf{k}+\mathbf{q}}$, one can simply obtain these effective band parameters through perturbation theory. For this purpose, we first perform a small- \mathbf{q} expansion of the Hamiltonian $H_{\mathbf{k}+\mathbf{q}} = H_{\mathbf{k}} + \sum_i q_i \partial H_{\mathbf{k}} / \partial k_i + (1/2) \sum_{ij} q_i q_j \partial^2 H_{\mathbf{k}} / (\partial k_i \partial k_j) + \dots$, and then treat all of the \mathbf{q} -dependent terms as a perturbative correction $V_{\mathbf{k}\mathbf{q}}$ to the unperturbed Hamiltonian $H_{\mathbf{k}}$, i.e., $H_{\mathbf{k}+\mathbf{q}} = H_{\mathbf{k}} + V_{\mathbf{k}\mathbf{q}}$, in the small \mathbf{q} limit. Assuming that $V_{\mathbf{k}\mathbf{q}}$ connects $|n\mathbf{k}\rangle$ state only to non-degenerate ones, thanks to the freedom in choosing a particular direction for \mathbf{q} , this approach gives $\varepsilon_{n,\mathbf{k}+\mathbf{q}} = \varepsilon_{n\mathbf{k}} + \langle n\mathbf{k} | V_{\mathbf{k}\mathbf{q}} | n\mathbf{k} \rangle + \sum' \frac{|\langle n\mathbf{k} | V_{\mathbf{k}\mathbf{q}} | n'\mathbf{k}' \rangle|^2}{\varepsilon_{n\mathbf{k}} - \varepsilon_{n'\mathbf{k}'}} + \dots$. Here, $\sum' \equiv \sum_{\{n'\mathbf{k}'\} \neq \{n\mathbf{k}\}}$ sums over all of the non-degenerate quantum states. By matching the coefficients of the linear and quadratic terms in \mathbf{q} , we eventually identify $\hbar v_{n\mathbf{k}}^i = \langle n\mathbf{k} | \partial H_{\mathbf{k}} / \partial k_i | n\mathbf{k} \rangle = \partial \varepsilon_{n\mathbf{k}} / \partial k_i$ as the effective band velocity, and

$$[\mathbb{M}_{n\mathbf{k}}^{-1}]^{ij} = \frac{1}{\hbar^2} \left\langle n\mathbf{k} \left| \frac{\partial^2 H_{\mathbf{k}}}{\partial k_i \partial k_j} \right| n\mathbf{k} \right\rangle + 2\text{Re} \sum' \frac{\langle n\mathbf{k} | \frac{\partial H_{\mathbf{k}}}{\partial k_i} | n'\mathbf{k}' \rangle \langle n'\mathbf{k}' | \frac{\partial H_{\mathbf{k}}}{\partial k_j} | n\mathbf{k} \rangle}{\hbar^2 (\varepsilon_{n\mathbf{k}} - \varepsilon_{n'\mathbf{k}'})} \quad (1)$$

as the inverse effective band mass tensor of the particle for the \mathbf{k} state. Here, Re denotes the real part of the resultant summation. In Eq. (1), while the first term on the right is due precisely to the intra-band contribution $[\mathbb{m}_{n\mathbf{k}}^{-1}]^{ij} = \partial^2 \varepsilon_{n\mathbf{k}} / (\hbar^2 \partial k_i \partial k_j)$ to the effective inverse mass tensor of the corresponding energy band, the second term is generated by the \mathbf{q} -induced virtual transitions.

Despite the use of perturbation theory in its derivation, Eq. (1) is exact, and in principle, the inter-band contribution need not necessarily be a small correction to the intra-band one. For instance, one can alternatively obtain Eq. (1) by taking the derivatives of the wave equation $H_{\mathbf{K}}|n\mathbf{K}\rangle = \varepsilon_{n\mathbf{K}}|n\mathbf{K}\rangle$ with respect

to $\mathbf{K} = \mathbf{k} + \mathbf{q}$ as follows. Using the orthonormalization condition $\langle n\mathbf{K} | n'\mathbf{K}' \rangle = \delta_{nn'} \delta(\mathbf{K} - \mathbf{K}')$ for the \mathbf{K} subspace of energy eigenstates, where $\delta_{nn'}$ is a Kronecker-delta and $\delta(x)$ is a Dirac-delta function, we first obtain $\langle n\mathbf{K} | \partial H_{\mathbf{K}} / \partial K_i | n'\mathbf{K}' \rangle = (\varepsilon_{n\mathbf{K}} - \varepsilon_{n'\mathbf{K}'}) \langle \partial n\mathbf{K} | \partial K_i | n'\mathbf{K}' \rangle + (\partial \varepsilon_{n\mathbf{K}} / \partial K_i) \delta_{nn'} \delta(\mathbf{K} - \mathbf{K}')$, leading to $\partial \varepsilon_{n\mathbf{K}} / \partial K_i = \langle n\mathbf{K} | \partial H_{\mathbf{K}} / \partial K_i | n\mathbf{K} \rangle$. Then, by taking the derivative of this expression with respect to K_j , i.e., $\partial^2 \varepsilon_{n\mathbf{K}} / (\partial K_i \partial K_j) = \langle n\mathbf{K} | \partial^2 H_{\mathbf{K}} / (\partial K_i \partial K_j) | n\mathbf{K} \rangle + \langle \partial n\mathbf{K} | \partial K_j | \partial H_{\mathbf{K}} / \partial K_i | n\mathbf{K} \rangle + \langle n\mathbf{K} | \partial H_{\mathbf{K}} / \partial K_i | \partial n\mathbf{K} / \partial K_j \rangle$, and using the completeness relation $\mathbb{I} = \sum_{n\mathbf{K}} |n\mathbf{K}\rangle \langle n\mathbf{K}|$ together with the derivative of the orthonormalization condition $(\partial \langle n\mathbf{K} | \partial K_i | n'\mathbf{K}' \rangle + \langle n\mathbf{K} | \partial n'\mathbf{K}' / \partial K_i \rangle) = 0$ for the \mathbf{K} subspace of interest, we eventually arrive at

$$\frac{\partial^2 \varepsilon_{n\mathbf{K}}}{\partial K_i \partial K_j} = \left\langle n\mathbf{K} \left| \frac{\partial^2 H_{\mathbf{K}}}{\partial K_i \partial K_j} \right| n\mathbf{K} \right\rangle + 2\text{Re} \sum' (\varepsilon_{n\mathbf{K}} - \varepsilon_{n'\mathbf{K}'}) \frac{\partial \langle n\mathbf{K} |}{\partial K_i} | n'\mathbf{K}' \rangle \langle n'\mathbf{K}' | \frac{\partial | n\mathbf{K} \rangle}{\partial K_j}. \quad (2)$$

This expression corresponds precisely to the coefficient $\hbar^2 [\mathbb{M}_{n\mathbf{k}}^{-1}]^{ij}$ of the quadratic term when $\mathbf{q} \rightarrow \mathbf{0}$, producing Eq. (1) without the use of perturbative approach.

Having established the theoretical framework on the effective band mass theorem for multi-band Hamiltonians, next we focus on two-band systems for their simplicity, and highlight not only the intriguing interpretation of the inter-band contribution from the quantum geometrical perspective but also illustrate its relative importance for a number of toy models that are of immediate experimental and/or theoretical interest.

Quantum metric of the projected Hilbert space. For this purpose, we note that the inter-band contribution to the effective band mass theorem given in Eq. (1) resembles closely, but not quite right, to the quantum metric $g_{n\mathbf{k}}^{ij}$ of the corresponding energy eigenstate. Recall that [37–39] $g_{n\mathbf{k}}^{ij} = \text{Re}(\partial \langle n\mathbf{k} | \partial k_i \rangle (\sum' |n'\mathbf{k}'\rangle \langle n'\mathbf{k}'|) (\partial |n\mathbf{k}\rangle / \partial k_j))$ is defined as the real part of the so-called quantum geometric tensor $Q_{n\mathbf{k}}^{ij} = g_{n\mathbf{k}}^{ij} - (i/2) F_{n\mathbf{k}}^{ij}$ of the projected Hilbert space, which can be equivalently expressed as $g_{n\mathbf{k}}^{ij} = \sum_{\mathbf{k}'} g_{n\mathbf{k}\mathbf{k}'}^{ij}$ where

$$g_{n\mathbf{k}\mathbf{k}'}^{ij} = \text{Re} \sum' \frac{\langle n\mathbf{k} | \frac{\partial H_{\mathbf{k}}}{\partial k_i} | n'\mathbf{k}' \rangle \langle n'\mathbf{k}' | \frac{\partial H_{\mathbf{k}}}{\partial k_j} | n\mathbf{k} \rangle}{(\varepsilon_{n\mathbf{k}} - \varepsilon_{n'\mathbf{k}'})^2}. \quad (3)$$

The geometrical importance of the quantum metric reveals itself as a measure of the quantum distance between differing quantum states, i.e., $ds_n^2 = \langle n\mathbf{k} | n\mathbf{k} \rangle - \langle n\mathbf{k} | n, \mathbf{k} + d\mathbf{k} \rangle = \sum_{\mu\nu} g_{n\mathbf{k}}^{ij} dk_i dk_j$. In contrast, the imaginary part $F_{n\mathbf{k}}^{ij}$ of the quantum geometric tensor is the Berry curvature, i.e., it is a distinct but related quantity corresponding to the emergent magnetic field in \mathbf{k} space.

Even though both $g_{n\mathbf{k}}^{ij}$ and $F_{n\mathbf{k}}^{ij}$ characterize the local \mathbf{k} -space geometry of the underlying quantum states,

they may also be linked with the global properties of the system in somewhat peculiar ways. For instance, the topological Chern invariant of a quantum-Hall system is determined by an integration of $F_{n\mathbf{k}}^{ij}$ in \mathbf{k} space, i.e., $2\pi C_n = \int_{BZ} dk_x dk_y F_{n\mathbf{k}}^{xy}$ controls the Hall conductivity [39]. Likewise, the superfluid density of some flat-band and two-band superfluids, that exhibit nontrivial quantum geometry, has a substantial contribution determined by an integration of $g_{n\mathbf{k}}^{ij}$ with a proper weight factor [31–33, 35]. Furthermore, by showing that the quantum metric contribution accounts for a sizeable fraction of the (Cooper) pair mass throughout the BCS-BEC crossover [33, 34], we have revealed the physical origin of its governing role in the superfluid density and hinted at its plausible roles in many other observables including the sound velocity and spin susceptibility [36]. Next we point out a distinct but related effect on the effective band mass of a single particle nearby the band minimum of the lower helicity band.

Effective band mass theorem for two-band Hamiltonians. We consider a generic two-band Hamiltonian density $H_{\mathbf{k}}$, and parametrize its energy eigenstates and eigenvalues with $|s\mathbf{k}\rangle$ and $\varepsilon_{s\mathbf{k}} = \varepsilon_{\mathbf{k}} + s d_{\mathbf{k}}$, respectively. Here, $s = \pm$ labels the upper/lower bands that are separated by a \mathbf{k} -dependent energy gap of $2d_{\mathbf{k}}$. When the geometric response is due only to the intermediate states from the differing band, i.e., $V_{\mathbf{k}\mathbf{q}}$ connects $|s\mathbf{k}\rangle$ to $|-s, \mathbf{k}'\rangle$ with $d_{\mathbf{k}} = d_{\mathbf{k}'} \neq 0$, thanks to the freedom in choosing a particular direction for \mathbf{q} , e.g., $\hat{\mathbf{q}} \perp \hat{\mathbf{k}}$ and $\hat{\mathbf{d}}_{\mathbf{q}} \perp \hat{\mathbf{d}}_{\mathbf{k}}$ in the toy models discussed below, a compact way to express the resultant effective band mass theorem for such a two-band system is

$$[\mathbb{M}_{s\mathbf{k}}^{-1}]^{ij} = [\mathbf{m}_{s\mathbf{k}}^{-1}]^{ij} + \frac{4s}{\hbar^2} d_{\mathbf{k}} g_{s\mathbf{k}}^{ij}. \quad (4)$$

Here, the usual intra-band contribution is simply denoted as $[\mathbf{m}_{s\mathbf{k}}^{-1}]^{ij}$, but the inter-band one is directly controlled by the quantum metric $g_{s\mathbf{k}\mathbf{k}'}^{ij} = \text{Re}(\partial\langle s\mathbf{k} | \partial k_i \rangle \langle -s, \mathbf{k}' | \partial k_j \rangle)$ of the corresponding quantum state. Note that the inter-band contributions have opposite signs for the $s = \pm$ bands.

Toy models for a spin-1/2 particle. To illustrate the relative importance of the inter-band contribution, next we consider a single spin-1/2 particle that is described by the generic Hamiltonian density $H_{\mathbf{k}} = \varepsilon_{\mathbf{k}} \sigma_0 + \mathbf{d}_{\mathbf{k}} \cdot \boldsymbol{\sigma}$, where $\varepsilon_{\mathbf{k}} = \hbar^2 k^2 / (2m_0)$ is the usual free-particle dispersion with m_0 the bare mass, and $\mathbf{d}_{\mathbf{k}} = \sum_i d_{\mathbf{k}}^i \hat{\mathbf{i}}$ is the SOC field with $\hat{\mathbf{i}}$ the unit vector along the i direction. Here, σ_0 is a 2×2 identity matrix, and $\boldsymbol{\sigma} = \sum_i \sigma_i \hat{\mathbf{i}}$ is a vector of Pauli spin matrices in such a way that $d_{\mathbf{k}}^i = \hbar \alpha_i k_i$ corresponds to the Weyl SOC when $\alpha_i = \alpha$ for all $i = \{x, y, z\}$, a Rashba SOC when $\alpha_z = 0$, and to an equal Rashba-Dresselhaus (ERD) SOC when $\alpha_y = \alpha_z = 0$. Here, we choose $\alpha \geq 0$ without the loss of generality. Note that $\varepsilon_{s\mathbf{k}} = \varepsilon_{\mathbf{k}} + s d_{\mathbf{k}}$ is the s -helicity dispersion with the following energy eigenstate

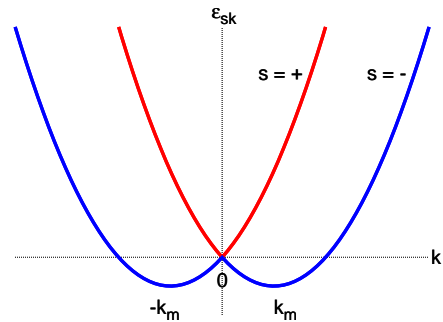


FIG. 1: (color online) By breaking the spin degeneracy of the particle dispersions $\varepsilon_{\sigma\mathbf{k}} = \varepsilon_{\mathbf{k}}$, the SOC $\mathbf{d}_{\mathbf{k}} \cdot \boldsymbol{\sigma}$ creates a pair of helicity bands $\varepsilon_{s\mathbf{k}} = \varepsilon_{\mathbf{k}} + s d_{\mathbf{k}}$. Here, $s = \pm$ corresponds to the upper/lower branches, and the figure illustrates them for a free particle $\varepsilon_{\mathbf{k}} = \hbar^2 k^2 / (2m_0)$ with Weyl SOC $d_{\mathbf{k}} = \hbar \alpha \mathbf{k}$. We are interested in the effective band mass of the particle nearby the band minimum (\mathbf{k}_m) of the lower helicity band.

$|s\mathbf{k}\rangle^T = (-d_{\mathbf{k}}^x + i d_{\mathbf{k}}^y, d_{\mathbf{k}}^z - s d_{\mathbf{k}}) / \sqrt{2d_{\mathbf{k}}(d_{\mathbf{k}} - s d_{\mathbf{k}}^z)}$, where $d_{\mathbf{k}} = |\mathbf{d}_{\mathbf{k}}|$ and T is the transpose operator. The quantum geometry is trivial for the ERD SOC as $g_{s\mathbf{k}\mathbf{k}'}^{ij} = 0$ for the entire \mathbf{k} space. It turns out that the quantum metrics of the $s = \pm$ bands are equal, e.g., $g_{s\mathbf{k}\mathbf{k}'}^{ij} = (\partial \hat{\mathbf{d}}_{\mathbf{k}} / \partial k_i) \cdot (\partial \hat{\mathbf{d}}_{\mathbf{k}'} / \partial k_j) / 4$, where $\hat{\mathbf{d}}_{\mathbf{k}} = \mathbf{d}_{\mathbf{k}} / d_{\mathbf{k}}$ is the unit vector along the SOC field. The equivalent expression $g_{s\mathbf{k}\mathbf{k}'}^{ij} = [\sum_{\ell} (\partial d_{\mathbf{k}}^{\ell} / \partial k_i) (\partial d_{\mathbf{k}'}^{\ell} / \partial k_j) - (\partial d_{\mathbf{k}} / \partial k_i) (\partial d_{\mathbf{k}'} / \partial k_j)] / (4d_{\mathbf{k}}^2)$ reduces simply to $g_{s\mathbf{k}\mathbf{k}'}^{ij} = \hbar^2 \alpha_i \alpha_j (d_{\mathbf{k}}^2 \delta_{ij} - d_{\mathbf{k}}^i d_{\mathbf{k}}^j) / (4d_{\mathbf{k}}^4)$.

Note that $g_{s\mathbf{k}\mathbf{k}'}^{ij} = 0$ in general for all \mathbf{k} states unless $\alpha_i \alpha_j \neq 0$, and that the geometric contribution to the relevant principal axes, i.e., $\hat{\mathbf{d}}_{\mathbf{q}} \perp \hat{\mathbf{d}}_{\mathbf{k}}$, can be written as $g_{s\mathbf{k}} \equiv \hbar^2 \alpha^2 (D - 1) / (4D d_{\mathbf{k}}^2)$, where $D = 3$ for the radial ($\hat{\mathbf{q}}$) direction of Weyl SOC with $d_{\mathbf{k}} = \hbar \alpha k$, $D = 2$ for the polar ($\mathbf{q}_{\perp} = q_x \hat{\mathbf{x}} + q_y \hat{\mathbf{y}}$) direction of Rashba SOC with $d_{\mathbf{k}} = \hbar \alpha k_{\perp}$, and $D = 1$ for the q_x direction of ERD SOC with $d_{\mathbf{k}} = \hbar \alpha |k_x|$. For instance, $g_{s\mathbf{k}\mathbf{k}'}^{xx} = (k_{\perp}^2 - k_x k'_x + k_y k'_y) / (8k_{\perp}^4)$, $g_{s\mathbf{k}\mathbf{k}'}^{yy} = (k_{\perp}^2 - k_y k'_y + k_x k'_x) / (8k_{\perp}^4)$, $g_{s\mathbf{k}\mathbf{k}'}^{xy} = g_{s\mathbf{k}\mathbf{k}'}^{yx} = -(k_x k'_y + k_y k'_x) / (8k_{\perp}^4)$, and the rest $g_{s\mathbf{k}\mathbf{k}'}^{iz} = g_{s\mathbf{k}\mathbf{k}'}^{zi} = 0$ vanishes for the Rashba SOC, and averaging over the degenerate \mathbf{k}'_{\perp} subspace with $k'_{\perp} = k_{\perp}$ leads to $g_{s\mathbf{k}} = 1 / (8k_{\perp}^2)$. Thus, in sharp contrast to the intra-band mass $m_{s\mathbf{k}} = m_0$ along the relevant principal axes $\hat{\mathbf{q}}$ [41], we find

$$\frac{M_{s\mathbf{k}}}{m_0} = \frac{D d_{\mathbf{k}}}{D d_{\mathbf{k}} + s(D - 1)m_0 \alpha^2}, \quad (5)$$

showing that the geometric contribution is negligible at large momentum, i.e., when $D d_{\mathbf{k}} \gg (D - 1)m_0 \alpha^2$. In this paper, we are interested in the effective band mass of the particle nearby the band minimum \mathbf{k}_m of the lower helicity band, e.g., the Weyl SOC is illustrated in Fig. 1. Plugging $k_m = m_0 \alpha / \hbar$ in Eq. (5), we find

$$M_{-,k_m} = D m_0, \quad (6)$$

where D is the dimensionality of the isotropic SOC field.

This analysis implies that the inter-band contribution to the effective band mass of the particle is a non-perturbative one for both Weyl and Rashba SOCs. In addition, this contribution is clearly independent of α at the band minimum as long as $\alpha \neq 0$. Furthermore, the dimensionality of the \mathbf{k} space does not play any role for the Rashba SOC, i.e., $M_{-,k_m}^\perp = 2m_0$ in both two and three dimensions. No matter how bizarre all of these rigorous results sound, we note that they are in excellent consistency with the effective mass M_{tb} of the relevant two-body bound states reported in the Fermi gas literature [42–49], where the binding occurs between an ($\uparrow; \mathbf{k} + \mathbf{q}/2$) particle and a ($\downarrow; -\mathbf{k} + \mathbf{q}/2$) one in the presence of a contact attraction. For instance, in Fig. 2, we reproduce M_{tb}^x as a function of the two-body binding energy E_{tb} in vacuum. In the non-interacting limit when $E_{tb} \rightarrow 0^+$, we clearly see that $M_{tb} = 6m_0$ for the Weyl SOC and $M_{tb}^\perp = 4m_0$ for the Rashba SOC as long as $\alpha \neq 0$, independently of its magnitude. In addition, it is also known that $M_{tb}^z = 2m_0$ for the Rashba SOC in three dimensions, and that the ERD SOC has no effect on the two-body problem. Thus, as M_{tb} coincides with twice the effective band mass of the particle at the band minimum of its lower helicity band, the geometric mass enhancement uncovers the mystery behind M_{tb} in the non-interacting limit. When E_{tb} increases from 0, however, a competing but distinct geometric effect on the bound state reduces M_{tb} towards the expected value $2m_0$ in the $E_{tb} \gg m_0\alpha^2$ limit [34].

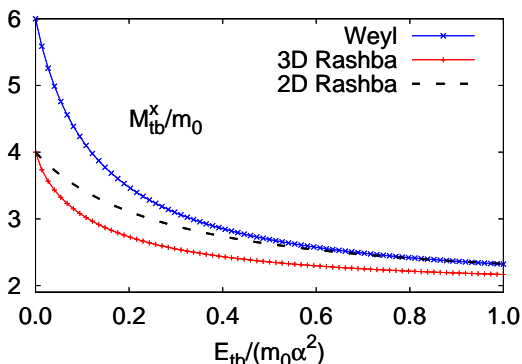


FIG. 2: (color online) The effective mass of the two-body bound state M_{tb}^x is shown for the Weyl and Rashba SOCs as a function of the two-body binding energy E_{tb} in vacuum [42–49]. In the non-interacting limit when $E_{tb} \rightarrow 0^+$, we note that M_{tb}^x approaches twice the effective band mass of the particle at the band minimum of its lower helicity band, i.e., $M_{tb} \rightarrow 2M_{-,k_m}$ in all cases considered here.

We note in passing that the electronic properties of some graphene-like solid-state materials are well-described by the low-energy Hamiltonian density $H_{\mathbf{k}} = \hbar\alpha\mathbf{k} \cdot \boldsymbol{\sigma}$, where α refers to the Fermi velocity, and $\boldsymbol{\sigma}$ refers not to the spin degrees of freedom of the electron but

to the sub-lattice degrees of freedom of the underlying crystal (i.e., honeycomb) lattice [14]. Since the helicity dispersions $\varepsilon_{sk} = s\alpha k$ are isotropic and linear in \mathbf{k} space, the intra-band contribution to the inverse effective mass vanishes along the radial ($\hat{\mathbf{q}}$) principal axis, suggesting that the effective band mass M_{sk} is determined solely by the inter-band contribution [50]. Thus, setting $m_0 \rightarrow \infty$ in Eq. (5) we find a linearly dispersing effective band mass

$$M_{sk} = \frac{sD}{D-1} \frac{\hbar k}{\alpha} \quad (7)$$

for the particles/holes in the upper/lower helicity bands, where $D \geq 2$ is the dimensionality of the \mathbf{k} space. Indeed, the long-established realization that the effective cyclotron mass $M_{sc} = s\hbar k_F/\alpha$ of the charge carriers in graphene has a strong $\sqrt{\rho}$ dependence in the low-density limit, provided one of the earliest smoking-gun evidences for the existence of a massless Dirac quasiparticle in the $k \rightarrow 0^+$ limit [12–14]. Here, $\rho = k_F^2/\pi$ is the electronic density of graphene with k_F the Fermi wave vector.

Conclusions. In summary, our so-called effective band mass theorem for the helicity bands has two physically distinct components: in addition to the usual contribution coming from the intra-band transitions, there exists a geometric contribution stemming from the virtual inter-band transitions. It turns out that the latter contribution is directly controlled by the quantum metric of the corresponding quantum state. To illustrate the relative importance of the inter-band contribution, we considered a spin-orbit coupled spin-1/2 particle, and calculated its effective band mass at the band minimum of the lower helicity band. We found that the bare mass m_0 of the particle jumps to $2m_0$ for the Rashba and to $3m_0$ for the Weyl coupling, independently of the coupling strength. We argued that such a geometric enhancement of the effective mass of the particle is in excellent consistency with the effective mass of the relevant two-body bound state in the non-interacting limit [42–49]. In addition, for graphene-like solid-state materials, we noted that the physical mechanism behind the linearly dispersing effective cyclotron mass of a Dirac quasiparticle [12–14] may be interpreted as a geometric mass acquisition.

The author thanks F. M. Ramazanoğlu and M. Ö. Okte1 for the critical reading of the manuscript, and acknowledges support from TÜBİTAK and the BAGEP award of the Turkish Science Academy.

-
- [1] Y.-J. Lin, K. Jiménez-García, and I. B. Spielman, “Spin-orbit-coupled Bose-Einstein condensates”, *Nature* **471**, 83 (2011).
 - [2] J. Y. Zhang, S. C. Ji, Z. Chen, L. Zhang, Z. D. Du, Bo Yan, G. S. Pan, B. Zhao, Y. J. Deng, H. Zhai, S. Chen, and J. W. Pan, “Collective Dipole Oscillations of a Spin-

- Orbit Coupled Bose-Einstein Condensate”, *Phys. Rev. Lett.* **109**, 115301 (2012).
- [3] P. Wang, Z.-Q. Yu, Z. Fu, J. Miao, L. Huang, S. Chai, H. Zhai, and J. Zhang, “Spin-orbit coupled degenerate Fermi gases”, *Phys. Rev. Lett.* **109**, 095301 (2012).
- [4] L. W. Cheuk, A.T. Sommer, Z. Hadzibabic, T. Yefsah, W. S. Bakr, and M.W. Zwierlein, “Spin-Injection Spectroscopy of a Spin-Orbit Coupled Fermi Gas”, *Phys. Rev. Lett.* **109**, 095302 (2012).
- [5] C. Qu, C. Hammer, M. Gong, C. Zhang, and P. Engels, “Observation of Zitterbewegung in a spin-orbit-coupled Bose-Einstein condensate”, *Phys. Rev. A* **88**, 021604(R) (2013).
- [6] A. J. Olson, S.-J. Wang, R. J. Niffenegger, C.-H. Li, C. H. Greene, and Y. P. Chen, “Tunable Landau-Zener transitions in a spin-orbit-coupled Bose-Einstein condensate”, *Phys. Rev. A* **90**, 013616 (2014).
- [7] K. Jiménez-García, L. LeBlanc, R. Williams, M. Beeler, C. Qu, M. Gong, C. Zhang, and I. Spielman, “Tunable Spin-Orbit Coupling via Strong Driving in Ultracold-Atom Systems”, *Phys. Rev. Lett.* **114**, 125301 (2015).
- [8] L. Huang, Z. Meng, P. Wang, P. Peng, S.-L. Zhang, L. Chen, D. Li, Q. Zhou, and J. Zhang, “Experimental realization of a two-dimensional synthetic spin-orbit coupling in ultracold Fermi gases”, *Nat. Phys.* **12**, 540 (2016).
- [9] Z. Meng, L. Huang, P. Peng, D. Li, L. Chen, Y. Xu, C. Zhang, P. Wang, and J. Zhang, “Experimental Observation of a Topological Band Gap Opening in Ultracold Fermi Gases with Two-Dimensional Spin-Orbit Coupling”, *Phys. Rev. Lett.* **117**, 235304 (2016).
- [10] Z. Wu, L. Zhang, W. Sun, X.-T. Xu, B.-Z. Wang, S.-C. Ji, Y. Deng, S. Chen, X.-J. Liu, and J.-W. Pan, “Realization of Two-Dimensional Spin-orbit Coupling for Bose-Einstein Condensates”, *Science* **354**, 83 (2016).
- [11] W. Sun, B.-Z. Wang, X.-T. Xu, C.-R. Yi, L. Zhang, Z. Wu, Y. Deng, X.-J. Liu, S. Chen, and J.-W. Pan, “Long-lived 2D Spin-Orbit coupled Topological Bose Gas”, *arXiv:1710.00717*.
- [12] K. S. Novoselov, A. K. Geim, S. V. Morozov, D. Jiang, M. I. Katsnelson, I. V. Grigorieva, S. V. Dubonos, and A. A. Firsov, “Two-dimensional gas of massless Dirac fermions in graphene”, *Nature* **438**, 197 (2005).
- [13] Y. Zhang, Y.-W. Tan, H. L. Stormer, and P. Kim, “Experimental observation of the quantum Hall effect and Berry’s phase in graphene”, *Nature* **438**, 201 (2005).
- [14] A. H. Castro Neto, F. Guinea, N. M. R. Peres, K. S. Novoselov, and A. K. Geim, “The electronic properties of graphene”, *Rev. Mod. Phys.* **81**, 109 (2009).
- [15] M. Z. Hasan and C. L. Kane, “Colloquium: Topological insulators”, *Rev. Mod. Phys.* **82**, 3045 (2010).
- [16] X.-L. Qi and S.-C. Zhang, “Topological insulators and superconductors”, *Rev. Mod. Phys.* **83**, 1057 (2011).
- [17] A. Kobayashi, S. Katayama, Y. Suzumura, and H. Fukuyama, “Massless Fermions in Organic Conductor”, *J. Phys. Soc. Jpn.* **76**, 034711 (2007).
- [18] L. Tarruell, D. Greif, T. Uehlinger, G. Jotzu, and Tilman Esslinger, “Creating, moving and merging Dirac points with a Fermi gas in a tunable honeycomb lattice”, *Nature* **483**, 302 (2012).
- [19] K. K. Gomes, W. Mar, W. Ko, F. Guinea, and H. C. Manoharan, “Designer Dirac fermions and topological phases in molecular graphene”, *Nature* **483**, 306 (2012).
- [20] M. Bellec, U. Kuhl, G. Montambaux, and F. Mortessagne, “Topological Transition of Dirac Points in a Microwave Experiment”, *Phys. Rev. Lett.* **110**, 033902 (2013).
- [21] N. Marzari and D. Vanderbilt, “Maximally localized generalized Wannier functions for composite energy bands”, *Phys. Rev. B* **56**, 12847 (1997).
- [22] P. Zanardi, P. Giorda, and M. Cozzini, “Information-Theoretic Differential Geometry of Quantum Phase Transitions”, *Phys. Rev. Lett.* **99**, 100603 (2007).
- [23] F. D. M. Haldane, “Geometrical Description of the Fractional Quantum Hall Effect”, *Phys. Rev. Lett.* **107**, 116801 (2011).
- [24] T. Neupert, C. Chamon, and C. Mudry, “Measuring the quantum geometry of Bloch bands with current noise”, *Phys. Rev. B* **87**, 245103 (2013).
- [25] T. S. Jackson, G. Moller, and R. Roy, “Geometric stability of topological lattice phases”, *Nat. Commun.* **6**, 8629 (2015).
- [26] Y. Gao, S. A. Yang, and Q. Niu, “Field Induced Positional Shift of Bloch Electrons and Its Dynamical Implications”, *Phys. Rev. Lett.* **112**, 166601 (2014).
- [27] M. Claassen, C. H. Lee, R. Thomale, X.-L. Qi, and T. P. Devereaux, “Position-Momentum Duality and Fractional Quantum Hall Effect in Chern Insulators”, *Phys. Rev. Lett.* **114**, 236802 (2015).
- [28] A. Srivastava and A. Imamoglu, “Signatures of Bloch-Band Geometry on Excitons: Nonhydrogenic Spectra in Transition-Metal Dichalcogenides”, *Phys. Rev. Lett.* **115**, 166802 (2015).
- [29] F. Piéchon, A. Raoux, J.-N. Fuchs, and G. Montambaux, “Geometric orbital susceptibility: Quantum metric without Berry curvature”, *Phys. Rev. B* **94**, 134423 (2016).
- [30] T. Ozawa, “Steady-state Hall response and quantum geometry of driven-dissipative lattices”, *Phys. Rev. B* **97**, 041108(R) (2018).
- [31] S. Peotta and P. Törmä, “Superfluidity in topologically nontrivial flat bands”, *Nat. Commun.* **6**, 8944 (2015).
- [32] A. Julku, S. Peotta, T. I. Vanhala, D.-H. Kim, and P. Törmä, “Geometric Origin of Superfluidity in the Lieb-Lattice Flat Band”, *Phys. Rev. Lett.* **117**, 045303 (2016).
- [33] M. Iskin, “Berezinskii-Kosterlitz-Thouless transition in the time-reversal-symmetric Hofstadter-Hubbard model”, *Phys. Rev. A* **97**, 013618 (2018).
- [34] M. Iskin, “Quantum metric contribution to the pair mass in spin-orbit coupled Fermi superfluids”, *arXiv:1801.09388*.
- [35] M. Iskin, “Exposing the quantum geometry of spin-orbit coupled Fermi superfluids”, *arXiv:1711.07262*.
- [36] M. Iskin, “Spin-susceptibility of spin-orbit coupled Fermi superfluids”, *arXiv:1802.03157*.
- [37] J. P. Provost and G. Vallee, “Riemannian structure on manifolds of quantum states”, *Commun. Math. Phys.* **76**, 289 (1980).
- [38] M. V. Berry, “The quantum phase, five years after in Geometric Phases in Physics”, edited by A. Shapere and F. Wilczek (World Scientific, Singapore, 1989).
- [39] D. J. Thouless, “Topological Quantum Numbers in Non-relativistic Physics”, (World Scientific, Singapore, 1998).
- [40] N. W. Ashcroft and N. D. Mermin, *Solid State Physics*, 1st ed. (Harcourt College Publishers, 1976).
- [41] Compare with the angular, i.e., polar and azimuthal for the Weyl and azimuthal for the Rashba SOC, directions of \mathbf{q} , where the intra-band effective mass of the particle $M_{sk}^{ang} = m_0 d_k / (d_k + s m_0 \alpha^2)$ remains intact, and $M_{-,km}$ diverges as the lower helicity band is flat for the degen-

- erate \mathbf{k}_m subspace.
- [42] Z.-Q. Yu and H. Zhai, “Spin-Orbit Coupled Fermi Gases across a Feshbach Resonance”, *Phys. Rev. Lett.* **107**, 195305 (2011).
- [43] M. Iskin and A. L. Subaşı, “Quantum phases of atomic Fermi gases with anisotropic spin-orbit coupling”, *Phys. Rev. A* **84**, 043621 (2011).
- [44] L. Jiang, X.-J. Liu, H. Hu, and H. Pu, “Rashba spin-orbit-coupled atomic Fermi gases”, *Phys. Rev. A* **84**, 063618 (2011).
- [45] H. Hu, L. Jiang, X.-J. Liu, and H. Pu, “Probing Anisotropic Superfluidity in Atomic Fermi Gases with Rashba Spin-Orbit Coupling”, *Phys. Rev. Lett.* **107**, 195304 (2011).
- [46] L. He and X.-G. Huang, “BCS-BEC Crossover in 2D Fermi Gases with Rashba Spin-Orbit Coupling”, *Phys. Rev. Lett.* **108**, 145302 (2012).
- [47] L. He and X.-G. Huang, “BCS-BEC crossover in three-dimensional Fermi gases with spherical spin-orbit coupling”, *Phys. Rev. B* **86**, 014511 (2012).
- [48] J. P. Vyasankere and V. B. Shenoy, “Rashbons: properties and their significance”, *New J. of Phys.* **14**, 043041 (2012).
- [49] J. P. Vyasankere and V. B. Shenoy, “Collective excitations, emergent Galilean invariance, and boson-boson interactions across the BCS-BEC crossover induced by a synthetic Rashba spin-orbit coupling”, *Phys. Rev. A* **86**, 053617 (2012).
- [50] Compare again with the angular directions of \mathbf{q} , where the intra-band effective mass of the particle $M_{sk}^{ang} = \hbar k/\alpha$ remains intact along the degenerate \mathbf{k} subspace.